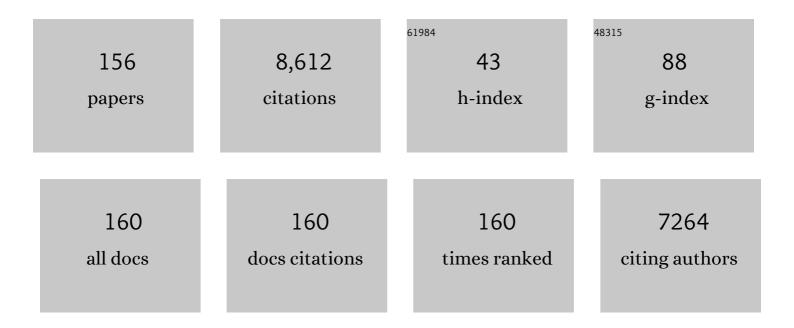
## Massimo Menenti

List of Publications by Year in descending order

Source: https://exaly.com/author-pdf/2000937/publications.pdf Version: 2024-02-01



#	Article	IF	CITATIONS
1	Quantifying spatial reallocation of land use/land cover categories in West Africa. Ecological Indicators, 2022, 135, 108556.	6.3	9
2	Calibration and Validation of SWAT Model by Using Hydrological Remote Sensing Observables in the Lake Chad Basin. Remote Sensing, 2022, 14, 1511.	4.0	21
3	Improved Parameterization of Snow Albedo in WRF + Noah: Methodology Based on a Severe Snow Event on the Tibetan Plateau. Advances in Atmospheric Sciences, 2022, 39, 1079-1102.	4.3	8
4	Quantification and Assessment of Global Terrestrial Water Storage Deficit Caused by Drought Using GRACE Satellite Data. IEEE Journal of Selected Topics in Applied Earth Observations and Remote Sensing, 2022, 15, 5001-5012.	4.9	6
5	Characterizing the thermal effects of vegetation on urban surface temperature. Urban Climate, 2022, 44, 101204.	5.7	7
6	Characterizing vegetation response to rainfall at multiple temporal scales in the Sahel-Sudano-Guinean region using transfer function analysis. Remote Sensing of Environment, 2021, 252, 112108.	11.0	18
7	Flood Extent Mapping in the Caprivi Floodplain Using Sentinel-1 Time Series. IEEE Journal of Selected Topics in Applied Earth Observations and Remote Sensing, 2021, 14, 5667-5683.	4.9	10
8	Challenges and Opportunities in Lidar Remote Sensing. Frontiers in Remote Sensing, 2021, 2, .	3.5	32
9	Anisotropy Parameterization Development and Evaluation for Glacier Surface Albedo Retrieval from Satellite Observations. Remote Sensing, 2021, 13, 1714.	4.0	10
10	Modeling the Underlying Drivers of Natural Vegetation Occurrence in West Africa with Binary Logistic Regression Method. Sustainability, 2021, 13, 4673.	3.2	4
11	Evapotranspiration estimates from an energy-water-balance model calibrated on satellite land surface temperature over the Heihe basin. Journal of Arid Environments, 2021, 188, 104466.	2.4	10
12	Nature-based solutions efficiency evaluation against natural hazards: Modelling methods, advantages and limitations. Science of the Total Environment, 2021, 784, 147058.	8.0	87
13	Improved parameterization of snow albedo in Noah coupled with Weather Research and Forecasting: applicability to snow estimates for the Tibetan Plateau. Hydrology and Earth System Sciences, 2021, 25, 4967-4981.	4.9	13
14	Assessing the impact of urban geometry on surface urban heat island using complete and nadir temperatures. International Journal of Climatology, 2021, 41, E3219.	3.5	15
15	Interannual and Seasonal Variability of Glacier Surface Velocity in the Parlung Zangbo Basin, Tibetan Plateau. Remote Sensing, 2021, 13, 80.	4.0	9
16	Optimal Estimate of Global Biome—Specific Parameter Settings to Reconstruct NDVI Time Series with the Harmonic ANalysis of Time Series (HANTS) Method. Remote Sensing, 2021, 13, 4251.	4.0	13
17	Combining multi-spectral and thermal remote sensing to predict forest fire characteristics. ISPRS Journal of Photogrammetry and Remote Sensing, 2021, 181, 400-412.	11.1	14
18	Glacier Area and Snow Cover Changes in the Range System Surrounding Tarim from 2000 to 2020 Using Google Earth Engine. Remote Sensing, 2021, 13, 5117.	4.0	8

#	Article	IF	CITATIONS
19	Multi-Source Hydrological Data Products to Monitor High Asian River Basins and Regional Water Security. Remote Sensing, 2021, 13, 5122.	4.0	3
20	Mapping Land Use Land Cover Transitions at Different Spatiotemporal Scales in West Africa. Sustainability, 2020, 12, 8565.	3.2	35
21	Unsupervised dimensionality reduction of hyperspectral images using representations of reflectance spectra. International Journal of Remote Sensing, 2020, 41, 7820-7845.	2.9	2
22	Change Detection Algorithm for Multi-Temporal Remote Sensing Images Based on Adaptive Parameter Estimation. IEEE Access, 2020, 8, 106083-106096.	4.2	11
23	Glacier Mass Balance in the Nyainqentanglha Mountains between 2000 and 2017 Retrieved from ZiYuan-3 Stereo Images and the SRTM DEM. Remote Sensing, 2020, 12, 864.	4.0	29
24	Development of spectral-phenological features for deep learning to understand Spartina alterniflora invasion. Remote Sensing of Environment, 2020, 242, 111745.	11.0	62
25	Aerosol characteristics and impacts on weather and climate over the Tibetan Plateau. National Science Review, 2020, 7, 492-495.	9.5	128
26	Adaptability of global olive cultivars to water availability under future Mediterranean climate. Mitigation and Adaptation Strategies for Global Change, 2019, 24, 435-466.	2.1	12
27	Detecting the Response of Irrigation Water Management to Climate by Remote Sensing Monitoring of Evapotranspiration. Water (Switzerland), 2019, 11, 2045.	2.7	5
28	Comparing Thresholding with Machine Learning Classifiers for Mapping Complex Water. Remote Sensing, 2019, 11, 1351.	4.0	89
29	Parameterization of Urban Sensible Heat Flux from Remotely Sensed Surface Temperature: Effects of Surface Structure. Remote Sensing, 2019, 11, 1347.	4.0	9
30	Glacier Facies Mapping Using a Machine-Learning Algorithm: The Parlung Zangbo Basin Case Study. Remote Sensing, 2019, 11, 452.	4.0	46
31	A numerical analysis of aggregation error in evapotranspiration estimates due to heterogeneity of soil moisture and leaf area index. Agricultural and Forest Meteorology, 2019, 269-270, 335-350.	4.8	8
32	Generating high-temporal and spatial resolution TIR image data. International Journal of Applied Earth Observation and Geoinformation, 2019, 78, 149-162.	2.8	5
33	Evaluation of WRF Modeling in Relation to Different Land Surface Schemes and Initial and Boundary Conditions: A Snow Event Simulation Over the Tibetan Plateau. Journal of Geophysical Research D: Atmospheres, 2019, 124, 209-226.	3.3	41
34	Relating Spatiotemporal Patterns of Forest Fires Burned Area and Duration to Diurnal Land Surface Temperature Anomalies. Remote Sensing, 2018, 10, 1777.	4.0	31
35	Evapotranspiration. , 2018, , 25-50.		2
36	The Digital Belt and Road program in support of regional sustainability. International Journal of Digital Earth, 2018, 11, 657-669.	3.9	28

#	Article	IF	CITATIONS
37	Regional surface soil heat flux estimate from multiple remote sensing data in a temperate and semiarid basin. Journal of Applied Remote Sensing, 2017, 11, 016028.	1.3	2
38	SigVox – A 3D feature matching algorithm for automatic street object recognition in mobile laser scanning point clouds. ISPRS Journal of Photogrammetry and Remote Sensing, 2017, 128, 111-129.	11.1	57
39	Assessment of Water Use in Pan-Eurasian and African Continents by ETMonitor with Multi-Source Satellite Data. IOP Conference Series: Earth and Environmental Science, 2017, 57, 012050.	0.3	3
40	Adaptability to future climate of irrigated crops: The interplay of water management and cultivars responses. A case study on tomato. Biosystems Engineering, 2017, 157, 45-62.	4.3	9
41	Evaluation of Methods for Aerodynamic Roughness Length Retrieval from Very High-Resolution Imaging LIDAR Observations over the Heihe Basin in China. Remote Sensing, 2017, 9, 63.	4.0	15
42	A Spectral Unmixing Method with Ensemble Estimation of Endmembers: Application to Flood Mapping in the Caprivi Floodplain. Remote Sensing, 2017, 9, 1013.	4.0	25
43	Remote Sensing for Crop Water Management: From ET Modelling to Services for the End Users. Sensors, 2017, 17, 1104.	3.8	160
44	Spectral region identification versus individual channel selection in supervised dimensionality reduction of hyperspectral image data. Journal of Applied Remote Sensing, 2017, 11, 1.	1.3	5
45	Estimation of subpixel snow sublimation from multispectral satellite observations. Journal of Applied Remote Sensing, 2017, 11, 1.	1.3	7
46	Early Drought Detection by Spectral Analysis of Satellite Time Series of Precipitation and Normalized Difference Vegetation Index (NDVI). Remote Sensing, 2016, 8, 422.	4.0	31
47	Estimation of Daily Solar Radiation Budget at Kilometer Resolution over the Tibetan Plateau by Integrating MODIS Data Products and a DEM. Remote Sensing, 2016, 8, 504.	4.0	22
48	Modeling and Reconstruction of Time Series of Passive Microwave Data by Discrete Fourier Transform Guided Filtering and Harmonic Analysis. Remote Sensing, 2016, 8, 970.	4.0	4
49	Observing the Response of Terrestrial Vegetation to Climate Variability Across a Range of Time Scales by Time Series Analysis of Land Surface Temperature. Remote Sensing and Digital Image Processing, 2016, , 277-315.	0.7	3
50	An optimization of parameter settings in HANTS for global NDVI time series reconstruction. , 2016, , .		4
51	Terrestrial water cycle in South and East Asia: Hydrospheric and cryospheric data products. , 2016, , .		Ο
52	Evaluation of ET data products: Parameterizations, rate limiting process and influential surface properties. , 2016, , .		0
53	Effects of Urban Geometry on Turbulent Fluxes: A Remote Sensing Perspective. IEEE Geoscience and Remote Sensing Letters, 2016, 13, 1767-1771.	3.1	8
54	Development of an improved urban emissivity model based on sky view factor for retrieving effective emissivity and surface temperature over urban areas. ISPRS Journal of Photogrammetry and Remote Sensing, 2016, 122, 30-40.	11.1	37

#	Article	IF	CITATIONS
55	On the performance of remote sensing time series reconstruction methods – A spatial comparison. Remote Sensing of Environment, 2016, 187, 367-384.	11.0	62
56	Observation and simulation of lakeâ€air heat and water transfer processes in a highâ€altitude shallow lake on the Tibetan Plateau. Journal of Geophysical Research D: Atmospheres, 2015, 120, 12327-12344.	3.3	47
57	Modeling Top of Atmosphere Radiance over Heterogeneous Non-Lambertian Rugged Terrain. Remote Sensing, 2015, 7, 8019-8044.	4.0	59
58	Estimation of Aerodynamic Roughness Length over Oasis in the Heihe River Basin by Utilizing Remote Sensing and Ground Data. Remote Sensing, 2015, 7, 3690-3709.	4.0	16
59	Reconstruction of global MODIS NDVI time series: Performance of Harmonic ANalysis of Time Series (HANTS). Remote Sensing of Environment, 2015, 163, 217-228.	11.0	187
60	Analyzing the Inundation Pattern of the Poyang Lake Floodplain by Passive Microwave Data. Journal of Hydrometeorology, 2015, 16, 652-667.	1.9	15
61	Modeling the effective emissivity of the urban canopy using sky view factor. ISPRS Journal of Photogrammetry and Remote Sensing, 2015, 105, 211-219.	11.1	71
62	Quantifying the impact of cloud cover on ground radiation flux measurements using hemispherical images. International Journal of Remote Sensing, 2015, 36, 5087-5104.	2.9	4
63	Modeling of Anthropogenic Heat Flux Using HJ-1B Chinese Small Satellite Image: A Study of Heterogeneous Urbanized Areas in Hong Kong. IEEE Geoscience and Remote Sensing Letters, 2015, 12, 1466-1470.	3.1	60
64	Study of the geometry effect on land surface temperature retrieval in urban environment. ISPRS Journal of Photogrammetry and Remote Sensing, 2015, 109, 77-87.	11.1	46
65	Multi-temporal, multi-sensor retrieval of terrestrial vegetation properties from spectral–directional radiometric data. Remote Sensing of Environment, 2015, 158, 311-330.	11.0	49
66	Comparison of MOD16 and LSA-SAF MSG evapotranspiration products over Europe for 2011. Remote Sensing of Environment, 2015, 156, 510-526.	11.0	151
67	Monitoring of Irrigation Schemes by Remote Sensing: Phenology versus Retrieval of Biophysical Variables. Remote Sensing, 2014, 6, 5815-5851.	4.0	24
68	Evaluating MERIS-Based Aquatic Vegetation Mapping in Lake Victoria. Remote Sensing, 2014, 6, 7762-7782.	4.0	29
69	Improved Surface Reflectance from Remote Sensing Data with Sub-Pixel Topographic Information. Remote Sensing, 2014, 6, 10356-10374.	4.0	19
70	Non-Vegetated Playa Morphodynamics Using Multi-Temporal Landsat Imagery in a Semi-Arid Endorheic Basin: Salar de Uyuni, Bolivia. Remote Sensing, 2014, 6, 10131-10151.	4.0	20
71	Assessing reliability of classification in the most informative spectral regions of hyperspectral images. IOP Conference Series: Earth and Environmental Science, 2014, 17, 012064.	0.3	0
72	Evaluation of Algorithms to estimate Daily Evapotranspiration from Instantaneous Measurements under All-sky Conditions. IOP Conference Series: Earth and Environmental Science, 2014, 17, 012133.	0.3	2

#	Article	IF	CITATIONS
73	Climate change, effective water use for irrigation and adaptability of maize: A case study in southern Italy. Biosystems Engineering, 2014, 128, 82-99.	4.3	26
74	Global sensitivity analysis of the spectral radiance of a soil–vegetation system. Remote Sensing of Environment, 2014, 145, 131-144.	11.0	56
75	Evaluation of a Linear Mixing Model to Retrieve Soil and Vegetation Temperatures of Land Targets. IOP Conference Series: Earth and Environmental Science, 2014, 17, 012272.	0.3	Ο
76	Parameterization of Surface Roughness Based on ICESat/GLAS Full Waveforms: A Case Study on the Tibetan Plateau. Journal of Hydrometeorology, 2013, 14, 1278-1292.	1.9	15
77	Geometric dependency of Tibetan lakes on glacial runoff. Hydrology and Earth System Sciences, 2013, 17, 4061-4077.	4.9	38
78	Mapping air temperature using time series analysis of LST: the SINTESI approach. Nonlinear Processes in Geophysics, 2013, 20, 513-527.	1.3	26
79	Automatic Estimation of Excavation Volume from Laser Mobile Mapping Data for Mountain Road Widening. Remote Sensing, 2013, 5, 4629-4651.	4.0	16
80	Assessing the sensitivity of two new indicators of vegetation response to water availability for drought monitoring. Proceedings of SPIE, 2012, , .	0.8	7
81	Analyzing the inundation patterns in Asia floodplains by passive microwave data. Proceedings of SPIE, 2012, , .	0.8	2
82	ICESat derived elevation changes of Tibetan lakes between 2003 and 2009. International Journal of Applied Earth Observation and Geoinformation, 2012, 17, 12-22.	2.8	157
83	Evaluation of Harmonic Analysis of Time Series (HANTS): impact of gaps on time series reconstruction. , 2012, , .		7
84	ACA Multiagent System for Satellite Image Classification. Advances in Intelligent and Soft Computing, 2012, , 93-100.	0.2	2
85	Preface "Observing and modeling the catchment scale water cycle". Hydrology and Earth System Sciences, 2011, 15, 597-601.	4.9	69
86	Scanning geometry: Influencing factor on the quality of terrestrial laser scanning points. ISPRS Journal of Photogrammetry and Remote Sensing, 2011, 66, 389-399.	11.1	276
87	Phenological response of vegetation to upstream river flow in the Heihe Rive basin by time series analysis of MODIS data. Hydrology and Earth System Sciences, 2011, 15, 1047-1064.	4.9	79
88	SkelTre. Visual Computer, 2010, 26, 1283-1300.	3.5	104
89	Parameterization of heat fluxes at heterogeneous surfaces by integrating satellite measurements with surface layer and atmospheric boundary layer observations. Advances in Atmospheric Sciences, 2010, 27, 328-336.	4.3	17
90	EAGLE 2006 – Multi-purpose, multi-angle and multi-sensor in-situ and airborne campaigns over grassland and forest. Hydrology and Earth System Sciences, 2009, 13, 833-845.	4.9	48

#	Article	IF	CITATIONS
91	Retrieval of small-relief marsh morphology from Terrestrial Laser Scanner, optimal spatial filtering, and laser return intensity. Geomorphology, 2009, 113, 12-20.	2.6	63
92	Separation of Ground and Low Vegetation Signatures in LiDAR Measurements of Salt-Marsh Environments. IEEE Transactions on Geoscience and Remote Sensing, 2009, 47, 2014-2023.	6.3	97
93	Modelling bioclimate by means of Fourier analysis of NOAAâ€AVHRR NDVI time series in Western Argentina. International Journal of Climatology, 2008, 28, 1175-1188.	3.5	9
94	Impact of rainfall anomalies on Fourier parameters of NDVI time series of northwestern Argentina. International Journal of Remote Sensing, 2008, 29, 1125-1152.	2.9	9
95	Analysis of the land surface heterogeneity and its impact on atmospheric variables and the aerodynamic and thermodynamic roughness lengths. Journal of Geophysical Research, 2008, 113, .	3.3	42
96	Multi-angular Thermal Infrared Observations of Terrestrial Vegetation. , 2008, , 51-93.		6
97	Retrieval of vegetation moisture indicators for dynamic fire risk assessment with simulated MODIS radiance. , 2007, , .		1
98	Retrieval of canopy moisture content for dynamic fire risk assessment using simulated MODIS bands. , 2007, , .		0
99	A field experiment on spectrometry of crop response to soil salinity. Agricultural Water Management, 2007, 89, 39-48.	5.6	40
100	Mapping mixed vegetation communities in salt marshes using airborne spectral data. Remote Sensing of Environment, 2007, 107, 559-570.	11.0	63
101	Determination of regional distributions and seasonal variations of land surface heat fluxes from Landsat-7 Enhanced Thematic Mapper data over the central Tibetan Plateau area. Journal of Geophysical Research, 2006, 111, n/a-n/a.	3.3	74
102	The use of MODIS-simulated spectral bands for monitoring plant water stress as a help for dynamic fire risk assessment. , 2006, , .		1
103	Accuracy Vs. Operability: a Case Study Over Barrax In The Context Of The DEMETER Project. AIP Conference Proceedings, 2006, , .	0.4	4
104	A Multi-Scales Surface Energy Balance System For Operational Actual Surface Evapotranspiration Monitoring. AIP Conference Proceedings, 2006, , .	0.4	4
105	Golden Day Comparison of Methods to Retrieve ET (Kc-NDVI, Kc-analytical, MSSEBS, METRIC). AIP Conference Proceedings, 2006, , .	0.4	6
106	Retrieval of aerosol optical thickness from PROBA-CHRIS images acquired over a coniferous forest. , 2005, 5976, 132.		0
107	Remote sensing parameterization of regional land surface heat fluxes over arid area in northwestern China. Journal of Arid Environments, 2004, 57, 257-273.	2.4	16
108	Understanding vegetation response to climate variability from space: recent advances towards the SPECTRA Mission. , 2004, , .		1

#	Article	IF	CITATIONS
109	Multi-angular hyperspectral observations of Mediterranean forest with PROBA-CHRIS. , 2004, , .		4
110	Remote sensing parameterization of land surface heat fluxes over arid and semi-arid areas. Advances in Atmospheric Sciences, 2003, 20, 530-539.	4.3	20
111	Assessment of climate impact on vegetation dynamics by using remote sensing. Physics and Chemistry of the Earth, 2003, 28, 103-109.	2.9	144
112	On measuring and remote sensing surface energy partitioning over the Tibetan Plateau––from GAME/Tibet to CAMP/Tibet. Physics and Chemistry of the Earth, 2003, 28, 63-74.	2.9	80
113	Estimation of sensible heat flux using the Surface Energy Balance System (SEBS) and ATSR measurements. Physics and Chemistry of the Earth, 2003, 28, 75-88.	2.9	137
114	Effective aerodynamic roughness estimated from airborne laser altimeter measurements of surface features. International Journal of Remote Sensing, 2003, 24, 1545-1558.	2.9	74
115	A practical algorithm to infer soil and foliage component temperatures from bi-angular ATSR-2 data. International Journal of Remote Sensing, 2003, 24, 4739-4760.	2.9	74
116	<title>Detection of main structures in digital images by expansion of border-containing windows</title> ., 2003, , .		0
117	Regionalization of Surface Fluxes over Heterogeneous Landscape of the Tibetan Plateau by Using Satellite Remote Sensing Data. Journal of the Meteorological Society of Japan, 2003, 81, 277-293.	1.8	38
118	Assimilation of land surface temperature data from ATSR in an NWP environment–a case study. International Journal of Remote Sensing, 2002, 23, 5193-5209.	2.9	13
119	Assessment of inputs to land surface processes models derived from hyperspectral multiangular data. , 2002, 4542, 223.		1
120	Simulation studies of long-term saline water use: model validation and evaluation of schedules. Agricultural Water Management, 2002, 54, 123-157.	5.6	43
121	Using the SIMGRO regional hydrological model to evaluate salinity control measures in an irrigation area. Agricultural Water Management, 2002, 56, 1-15.	5.6	9
122	Determination of Regional Land Surface Heat Flux Densities over Heterogeneous Landscape of HEIFE Integrating Satellite Remote Sensing with Field Observations Journal of the Meteorological Society of Japan, 2002, 80, 485-501.	1.8	30
123	Determination of regional net radiation and soil heat flux over a heterogeneous landscape of the Tibetan Plateau. Hydrological Processes, 2002, 16, 2963-2971.	2.6	61
124	Relating satellite multiangular thermal infrared observations to soil and foliage temperature. Advances in Space Research, 2002, 30, 2529-2533.	2.6	3
125	Indicators of the Seasonal Cycle of Total Dissolved and Adsorbed Salts under Irrigation. Water Resources Management, 2002, 16, 89-103.	3.9	4
126	Modeling sensible heat flux using estimates of soil and vegetation temperatures: the HEIFE and IMGRASS experiments. Advances in Global Change Research, 2001, , 23-49.	1.6	5

#	Article	IF	CITATIONS
127	Estimation of soil and vegetation temperatures with multiangular thermal infrared observations: IMGRASS, HEIFE, and SGP 1997 experiments. Journal of Geophysical Research, 2001, 106, 11997-12010.	3.3	48
128	S-SEBI: A simple remote sensing algorithm to estimate the surface energy balance. Physics and Chemistry of the Earth, 2000, 25, 147-157.	0.3	540
129	Mapping vegetation-soil-climate complexes in southern Africa using temporal Fourier analysis of NOAA-AVHRR NDVI data. International Journal of Remote Sensing, 2000, 21, 973-996.	2.9	167
130	Reconstructing cloudfree NDVI composites using Fourier analysis of time series. International Journal of Remote Sensing, 2000, 21, 1911-1917.	2.9	484
131	Aggregation effects of surface heterogeneity in land surface processes. Hydrology and Earth System Sciences, 1999, 3, 549-563.	4.9	75
132	Regional application of one-dimensional water flow models for irrigation management. Agricultural Water Management, 1999, 40, 291-302.	5.6	45
133	Mapping isogrowth zones on continental scale using temporal Fourier analysis of AVHRR-NDVI data. International Journal of Applied Earth Observation and Geoinformation, 1999, 1, 9-20.	2.8	16
134	Assimilation of multispectral measurements in interactive land surface models. Advances in Space Research, 1998, 22, 611-624.	2.6	1
135	A remote sensing surface energy balance algorithm for land (SEBAL). 1. Formulation. Journal of Hydrology, 1998, 212-213, 198-212.	5.4	2,175
136	Area-average estimates of evaporation, wetness indicators and top soil moisture during two golden days in EFEDA. Agricultural and Forest Meteorology, 1997, 87, 119-137.	4.8	44
137	The use of hydrological models in the irrigated areas of Mendoza, Argentina. Agricultural Water Management, 1997, 35, 11-28.	5.6	8
138	Relating Crop Water Consumption to Irrigation Water Supply by Remote Sensing. Water Resources Management, 1997, 11, 445-465.	3.9	65
139	Remote Sensing, GIS and Hydrological Modelling for Irrigation Management. , 1996, , 453-472.		5
140	Cover A colour composite of NOAA-AVHRR-NDVI based on time series analysis (1981-1992). International Journal of Remote Sensing, 1996, 17, 231-235.	2.9	124
141	Modeling Spatial Sediment Delivery in an Arid Region Using Thematic Mapper Data and GIS. Transactions of the American Society of Agricultural Engineers, 1996, 39, 551-557.	0.9	4
142	Performance indicators for the statistical evaluation of digital image classifications. ISPRS Journal of Photogrammetry and Remote Sensing, 1996, 51, 78-90.	11.1	17
143	Measurements of land surface features using an airborne laser altimeter: the HAPEX-Sahel experiment. International Journal of Remote Sensing, 1996, 17, 3705-3724.	2.9	22
144	Remote Sensing Parameterization of Meso-scale Land Surface Evaporation. , 1996, , 401-429.		6

9

#	Article	IF	CITATIONS
145	The Scaling-up of Processes in the Heterogeneous Landscape of HEIFE with the Aid of Satellite Remote Sensing. Journal of the Meteorological Society of Japan, 1995, 73, 1235-1244.	1.8	54
146	Fourier analysis of time series of NOAA-AVHRR NDVI composites to map isogrowth zones. Studies in Environmental Science, 1995, 65, 425-430.	0.0	3
147	A user-oriented and quantifiable approach to irrigation design. Water Resources Management, 1995, 9, 95-113.	3.9	7
148	Estimation of effective aerodynamic roughness of Walnut Gulch watershed with laser altimeter measurements. Water Resources Research, 1994, 30, 1329-1337.	4.2	107
149	Understanding land surface evapotranspiration with satellite multispectral measurements. Advances in Space Research, 1993, 13, 89-100.	2.6	21
150	Mapping agroecological zones and time lag in vegetation growth by means of fourier analysis of time series of NDVI images. Advances in Space Research, 1993, 13, 233-237.	2.6	168
151	Is large-scale inverse modelling of unsaturated flow with areal average evaporation and surface soil moisture as estimated from remote sensing feasible?. Journal of Hydrology, 1993, 143, 125-152.	5.4	74
152	Appraisal and optimization of agricultural water use in large irrigation schemes: I. Theory. Water Resources Management, 1992, 6, 185-199.	3.9	5
153	Appraisal and optimization of agricultural water use in large irrigation schemes: II. Applications. Water Resources Management, 1992, 6, 201-221.	3.9	6
154	Linear relationships between surface reflectance and temperature and their application to map actual evaporation of groundwater. Advances in Space Research, 1989, 9, 165-176.	2.6	54
155	Determination of surface hemispherical reflectance with Thematic Mapper data. Remote Sensing of Environment, 1989, 28, 327-337.	11.0	37
156	HYDROLOGIC AND CRYOSPHERIC PROCESSES OBSERVED FROM SPACE. International Archives of the Photogrammetry, Remote Sensing and Spatial Information Sciences - ISPRS Archives, 0, XL-7/W3, 1101-1110.	0.2	3